Structural and Surface Characterization of Pure and Sulfated Iron Oxides

Giuliana Magnacca,*,† Giuseppina Cerrato,† Claudio Morterra,†
Michela Signoretto,‡ Filippo Somma,‡ and Francesco Pinna‡

Dipartimento di Chimica IFM, Università di Torino, Via P. Giuria 7, I-10125 Torino, Italy, and Dipartimento di Chimica, Università di Venezia, Calle Larga S. Marta 2137, I-30123 Venezia, Italy

Received July 19, 2002. Revised Manuscript Received November 22, 2002

Iron oxide catalysts, pure and surface-doped with variable amounts of sulfate groups, have been prepared and characterized by means of electron microscopy (HR-TEM), N_2-adsorption at 77 K (BET area and porosity), X-ray diffraction (XRD), adsorption microcalorimetry, and various spectroscopic techniques (UV−Vis, Raman, and FTIR). The catalysts were prepared from aqueous solutions of ammonia and iron nitrate, with production of an amorphous precipitate that transformed into α-Fe_2O_3 upon calcination at 773 K. The sulfation of iron oxide was carried out by adding two dosed amounts of aqueous $(NH_4)_2SO_4$ to the starting hydroxide, as normally done for the preparation of other sulfated oxidic catalysts. Nominal sulfate loadings of 2 and 8 wt % were obtained, corresponding to ∼1.4 and ∼4.1 sulfate groups per nm^2, respectively. The use of various experimental techniques allowed the description of the morphological and structural aspects of the systems, whereas in-situ IR spectroscopy of adsorbed probe-molecules (e.g., CO, CO_2, and 2,6-dimethylpyridine) and the combined use of IR spectroscopy and microcalorimetry of CO adsorption at room temperature were used to characterize surface acidity and basicity. TEM, XRD, and BET measurements indicate that the presence of sulfate groups does not modify the crystalline structure of α-Fe_2O_3, but decreases crystallites size and, consequently, increases specific surface area. The presence of sulfates increases the strength of surface Lewis acidity, but the overall amount of Lewis acid sites decreases, while few Brønsted acidic sites of medium-low strength are produced. Surface basicity of iron oxide, mainly tested by the adsorption of CO_2 and formation of surface carbonate-like species, is gradually decreased by sulfates, but not suppressed. The vacuum reducibility of iron oxide (which can be spectroscopically evidenced both by a color change (UV−Vis spectra) and by the formation, upon CO adsorption, of surface carbonyl-like species with a π-back-donation component (IR spectra)) turns out to be dramatically hindered by the presence of surface sulfates.

Introduction

Iron oxide based systems find application in the design of electromagnetic devices, pigments, and photosensitive materials.[1] Since the early 1980s, great attention has been directed toward the class of sulfated metal oxides because of their activity in various acid-catalyzed reactions[2−4].

Maximum effort so far has been devoted to investigating the catalytic activity of sulfated zirconia-based systems.[5] Sulfated iron oxide has been reported to exhibit catalytic activity in several reactions, including the dehydration of alcohols[6,7] and the partial oxidation of methane,[8] for which one tries to combine the hydrocarbon activation properties (typical of acidic systems) with the redox behavior of iron oxide. In particular, it seems that sulfate ions may inhibit domain grain growth by restricting cationic mobility (the transformation of goethite into haematite involves the rearrangement of cations) and thus stabilizing the surface area of iron oxide. Moreover, sulfation should suppress the low-temperature total oxidation, and enhance the production of selective oxidation products, by selectively blocking Fe^{3+} oxidation sites.[9]

Few papers present in the literature deal with catalytic systems based on iron oxide. Some of them consider the effects of different precursors of Fe_2O_3[1], or the effect of different sulfating agents (see ref. 10 and references

* To whom inquiries may be addressed. Phone: +39 011 6707543. Fax: +39 011 6707855. E-mail: giuliana.magnacca@unito.it.
† Università di Torino.
‡ Università di Venezia.

(1) Wong, S. S.; Brus, L. E. *J. Phys. Chem. B* **2001**, *105* (3), 599.
(2) Hino, M.; Arata, K. *Chem. Lett.* **1979**, 1259.
(3) Olah, G. A.; Prakash, G. K. S.; Sommer, J. *Superacids*; Wiley: New York, 1985; p 53.
(4) Arata, K.; Hino, M. *Mater. Chem. Phys.* **1990**, *26*, 213.
(5) Song, X.; Sayari, A. *Catal. Rev. Sci. Eng.* **1996**, *38* (3), 329.
(6) Tanabe, K.; Kayo, A.; Yamaguchi, T. *J. Catal.* **1983**, *83*, 99.
(7) Comelli, R. A.; Vera, C. R.; Parera, J. M. *J. Catal.* **1995**, *151*, 96.
(8) Brown, A. S. C.; Hargreaves, J. S. J.; Rijniersce, B. *Catal. Today* **1998**, *45*, 47.
(9) Brown, A. S. C.; Hargreaves, J. S. J.; Rijniersce, B. *Catal. Lett.* **1998**, *53*, 7.
(10) Yamaguchi, T.; Jin, T.; Tanabe, K. *J. Phys. Chem.* **1986**, *90*, 3148.

10.1021/cm021268n CCC: $25.00
Published on Web 01/17/2003

therein) on the catalytic activity of iron oxide. The aim of the present work is a preliminary characterization of pure and sulfated Fe_2O_3, to be possibly used in some industrial applications. Some already tested characterization methods, previously applied to the study of sulfated zirconia systems, were used also in the present case.

Experimental Section

Materials. Pure and sulfated iron oxide systems were prepared using a procedure similar to that previously adopted by Tanabe et al. and described in reference 6. $Fe(NO_3)_3 \cdot 9H_2O$ (Sigma, minimum purity 98%) was dissolved at room temperature (RT) in aqueous NH_3 (Carlo Erba, 30% solution) at pH 8 under vigorous stirring. The precipitate was aged in the mother liquor overnight, then carefully washed with warm water (T = 333 K), filtered, and oven-dried overnight at 383 K to obtain a fine $Fe(OH)_3$ powder.

Sulfation was carried out on the dried $Fe(OH)_3$ powder by impregnation with different amounts of aqueous $(NH_4)_2SO_4$ (Sigma, minimum purity 99.0%), so as to obtain two nominal SO_4^{2-} loadings (i.e., 2 and 8 wt %, respectively).

Sulfated and nonsulfated iron hydroxides were then calcined at 773 K in a dry air flow for 3h to obtain the desired α-Fe_2O_3 phase, as indicated by XRD analysis.

Methods. Preliminary TG-DTA runs were performed on the precursor materials, to evidence the temperature of transformation into the hematite phase. The measurements were carried out using a simultaneous thermal analyzer (STA 429, Netzsch). All samples (150 mg) were first dried for 12 h at 383 K, and then heated at linear rate (10 K/min) from 298 to 1223 K in a dry air flow (30 mL/min).

Sulfate analysis on calcined materials was carried out by ion chromatography, as reported elsewhere.[11] In the present case the data refer to the amount of sulfates actually present at the surface of the materials because the analysis was carried out on the extracting basic solution, after thorough washing of the powders.

BET surface areas and pore size distributions (BJH method) were obtained by N_2 adsorption/desorption at 77 K, using an ASAP2010 automatic instrument (Micromeritics).

X-ray diffraction data were obtained with a Philips PW 1830 diffractometer in a standard Bragg−Brentano geometry (Co K_α radiation).

Raman spectra were obtained at 4 cm^{-1} resolution using a FRA 106/RFS 100 FT spectrophotometer (Bruker), equipped with a Nd:YAG laser (near-IR emission and power in the 0−300 mW range) and with a Ge detector (D418-S).

TEM and (HR)TEM images were obtained with a JEOL electron microscope (JEM 2000EX model, operating at 200 kV), equipped with a top-entry stage, polepiece, and LaB_6 filament. All samples were supported by dry dispersion onto Cu grids covered with a "holey" carbon film.

Temperature programmed reduction (TPR) measurements were performed in a standard apparatus, previously described.[12] The calcined samples were heated at a linear rate (10 K/min) from 298 to 773/1273 K in a gas mixture composed by 5% H_2 in Ar, 40 mL in STP.

FTIR spectra were obtained at 4 cm^{-1} resolution with a Bruker IFS 113v spectrophotometer equipped with MCT cryodetector. Unless otherwise specified, the samples were inspected in the form of self-supporting pellets of ~50 mg/cm^2, and were thermally activated in situ in a conventional glass vacuum line (residual pressure < 10^{-5} Torr). When dealing with optically thick or highly scattering systems, the samples were inspected in the form of thin-layer depositions on a Si wafer of ~20 mg/cm^2, and were activated in situ, as in the case of pellet samples.

Volumetric isotherms and energetic features of CO adsorption at 303 K were carried out in a microcalorimeter (Tian-Calvet type, by Setaram) equipped with a calibrated glass gas-volumetric apparatus, where absolute pressures were measured by a Barocell gauge (Edwards, range 0−100 Torr).

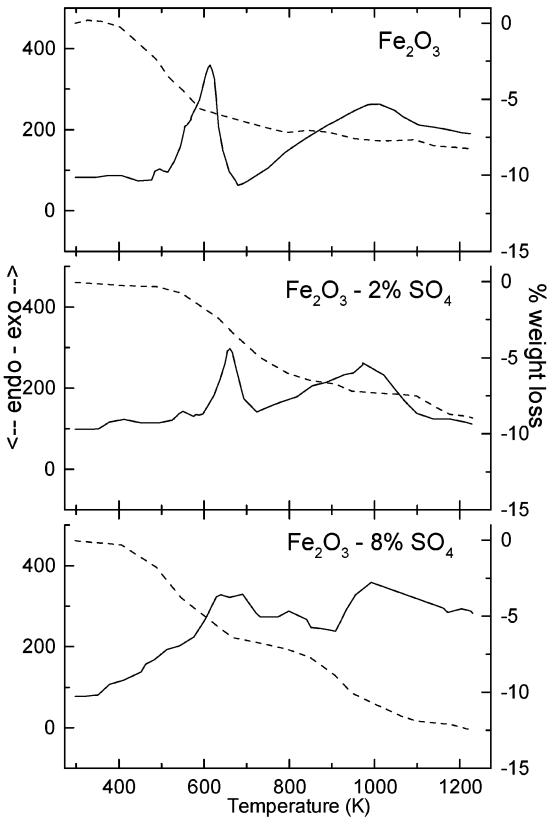

Figure 1. TG-DTA results in the temperature range 293−1223 K for Fe_2O_3 (upper curves), Fe_2O_3 2% SO_4 (intermediate curves), and Fe_2O_3 8% SO_4 (lower curves). Broken-line traces are relative to TGA curves (% weight loss, right ordinate), solid-line traces are relative to DTA curves (ΔT, left ordinate).

Results and Discussion

TG-DTA Analysis. Starting from the dried $Fe(OH)_3$ precursor, and increasing the vacuum-treatment temperature, all the transformations occurring on iron oxide systems could be observed. The effects of heating, from RT to 1223 K, are reported in Figure 1 for all samples of interest.

The transformations expected to occur on the dried starting amorphous compound are summarized in the following scheme, where each stage should bring about a loss of water:

$$\text{(dry) } Fe(OH)_3 \rightarrow (\alpha\text{-FeOOH (goethite)}) \rightarrow \alpha\text{-}Fe_2O_3 \text{ (hematite)}$$

Each stage should also occur with changes in the thermal response of the material, as normally witnessed by typical λ-shaped peaks.

All DTA curves show a pronounced exothermic peak at ~600 K, representing the phase transition from amorphous $Fe(OH)_3$ to crystalline hematite.[13] In each case, the peak is accompanied by an appreciable weight loss due to water elimination. The temperature of phase

(11) Sarzanini, C.; Sacchero, G.; Pinna, F.; Signoretto, M.; Cerrato, G.; Morterra, C. *J. Mater. Chem.* **1995**, *5*, 353.
(12) Dall'Agnol, C.; Gervasini, A.; Morazzoni, F.; Pinna, F.; Strukul, G.; Zanderighi, L. *J. Catal.* **1985**, *96*, 106.

Table 1. Nominal and Real Coverage of Sulfate Groups (Reported as wt % and Groups per nm^2), Specific Surface Area, and Porosity of Pure and Sulfated Iron Oxides

sample	$[SO_4^{2-}]$ wt % nominal	$[SO_4^{2-}]$ wt % measured[a]	SO_4^{2-} groups per nm^2	BET specific surface area[b] (m^2/g)	BJH total porosity[c] (cm^3/g)
Fe_2O_3				25	0.112
Fe_2O_3 2% SO_4	2%	1.50%	1.6	50	0.168
Fe_2O_3 8% SO_4	8%	5.80%	4.6	74	0.193

[a] From ref 11. [b] From ref 15. [c] From ref 16.

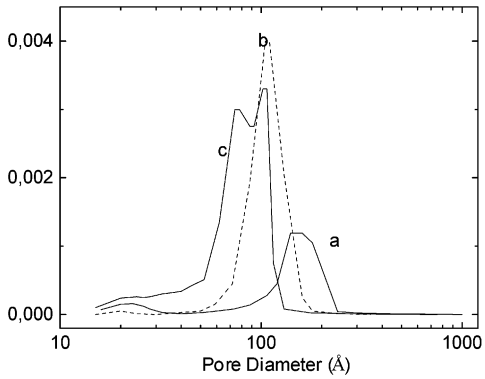

Figure 2. Pore size distribution measured by means of N_2 adsorption/desorption at 77 K for Fe_2O_3 (curve a), Fe_2O_3 2% SO_4 (curve b), and Fe_2O_3 8% SO_4 (curve c). The distribution curves reported are relative to the desorption branch of the isotherms.

transformation varies with sulfates loading: the increase of sulfates loading brings about an appreciable increase of the transition temperature, and renders the peak less and less sharp.[14]

At higher temperatures (~1000 K) another exothermic signal is visible, associated with an appreciable weight loss only for sulfated systems. It should be related to a further phase transition which, in the case of sulfated systems, occurs with the (exothermic) decomposition of sulfates, starting from a temperature of ~800 K.

On the basis of these data, we chose to treat the amorphous precursors at 773 K in an oxidizing atmosphere, to obtain in all cases the desired α-Fe_2O_3 phase, with an amount of sulfates as large as possible.

Sulfate Contents, Specific Surface Areas, and Porosity. Sulfate coverages, as well as specific surface areas and porosity features are reported in Table 1.

The effect of sulfation on the specific surface area of α-Fe_2O_3 is clearly visible, and consistent with previous data.[9] As in the case of sulfated zirconia systems, the presence of sulfate groups at the surface of the oxide delays the growth of particles. At the same time, the increase of sulfates content brings about a continuous decrease of the average pore diameter, as indicated by the pore distribution curves reported in Figure 2. In particular, a much broader and (apparently) bimodal distribution of mesopores is obtained for the 8%-sulfated system, in which pore diameters are distributed between ~70 and ~100 Å.

Structural Characterization. Pure and sulfated iron oxides were studied by XRD (Figure 3) and Raman spectroscopy (Figure 4), to obtain information on the structural features of the materials. In particular, the scattering nature of the Raman spectroscopic technique should yield information mainly concerning the outermost layers of the particles, whereas XRD measurements should evidence the bulk structure of the materials.

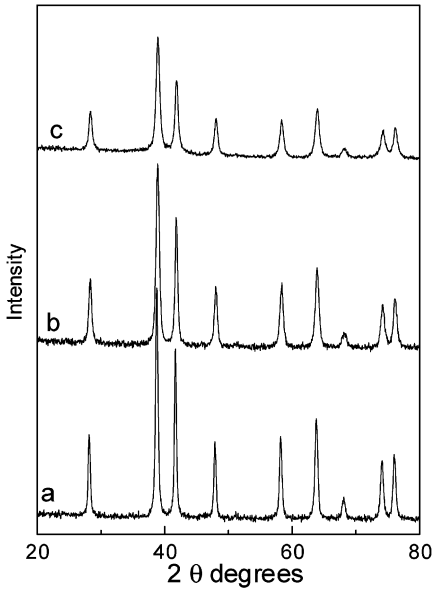

Figure 3. XRD patterns: Fe_2O_3, curve a; Fe_2O_3 2% SO_4, curve b; Fe_2O_3 8% SO_4, curve c.

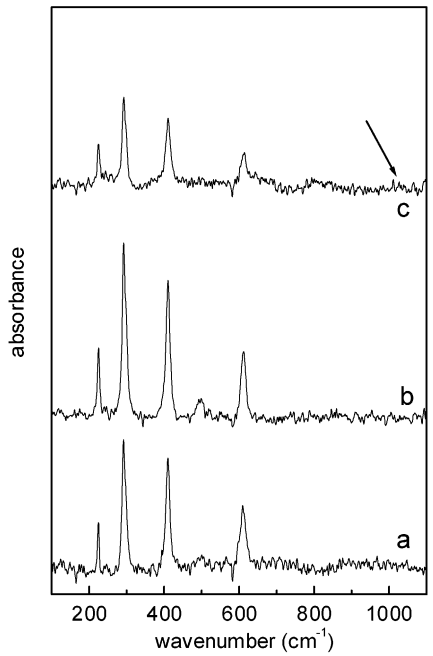

Figure 4. Raman spectra: Fe_2O_3, curve a; Fe_2O_3 2% SO_4, curve b; Fe_2O_3 8% SO_4, curve c. The arrow indicates the spectral position at which Raman band(s) due to sulfate groups should be expected.

(13) Mackenzie, R. C. *Differential Thermal Analysis*; Academic Press: London, 1970; Vol. I; pp 272−279.
(14) Arata, K. *Adv. Catal.* **1990**, *37*, 165.

In both cases the data indicate that pure and sulfated Fe_2O_3 are crystalline, and belong to the α-Fe_2O_3 (hematite) phase.[17]

Unexpectedly, in Raman spectra b and c of Figure 4 there is no spectral evidence for the presence of surface sulfates. This may be due to the low specific intensity of the Raman signal of sulfates, as suggested by Scheithauer et al.,[18] or to the low stability of surface sulfates in the laser beam, as suggested by one of the reviewers of this manuscript. Still, other oxidic systems loaded with comparable amounts of sulfates, characterized by a thermal stability similar to that of sulfates on Fe_2O_3, have been reported to present a broad and rather complex Raman band at $\sim$1000 cm^{-1}.[18−20]

It is interesting to consider the half-height-width of the XRD signals in Figure 3: on increasing the amount of sulfates, the peaks become gradually broader, indicating a smaller particle size (or, in other words, a gradual loss of crystalline order). This is consistent with data from BET surface area measurements (Table 1). Also the Raman spectrum of Figure 4c confirms that, on increasing the sulfates loading, the vibrational modes at $\bar{\nu} > 200$ cm^{-1}, analytical of the α-Fe_2O_3 phase, become shallow and poorly defined.

Morphological Characterization (TEM Analysis). By means of electron microscopy we can see directly the dimension of the particles, and the morphological features of the samples.

Figure 5, part A, shows that pure Fe_2O_3 is made up of crystalline acicular particles (60−70-nm length), with well-defined edges. In the presence of 8% sulfates (Figure 5, part B), the particles become less defined in shape and smaller in size (the average particle size becomes $\sim$20−30 nm), and also the porous texture of the material seems to become visible.

For both samples, the image analysis provides evidence of a far predominant diffraction fringe pattern ($d_{hkl} = 3.68$ Å), ascribable to the (102) crystal plane of α-Fe_2O_3.[21]

Reducibility of Samples: TPR Analysis. Figure 6 presents the TPR profiles relative to the three materials under study. Curve a, relative to pure α-Fe_2O_3, shows two maxima centered at $\sim$649 and $\sim$900 K, which are ascribed to the two-stages reduction of Fe_2O_3 to Fe^0, passing through the spinel-phase Fe_3O_4 (magnetite).[22]

When sulfates are present in a large amount (curve c), the first reduction signal of α-Fe_2O_3 shifts to higher temperatures ($\sim$673 K), indicating an increased reducibility threshold. For both sulfated systems, the second reduction signal, located at higher temperatures, is complex and much more difficult to interpret because

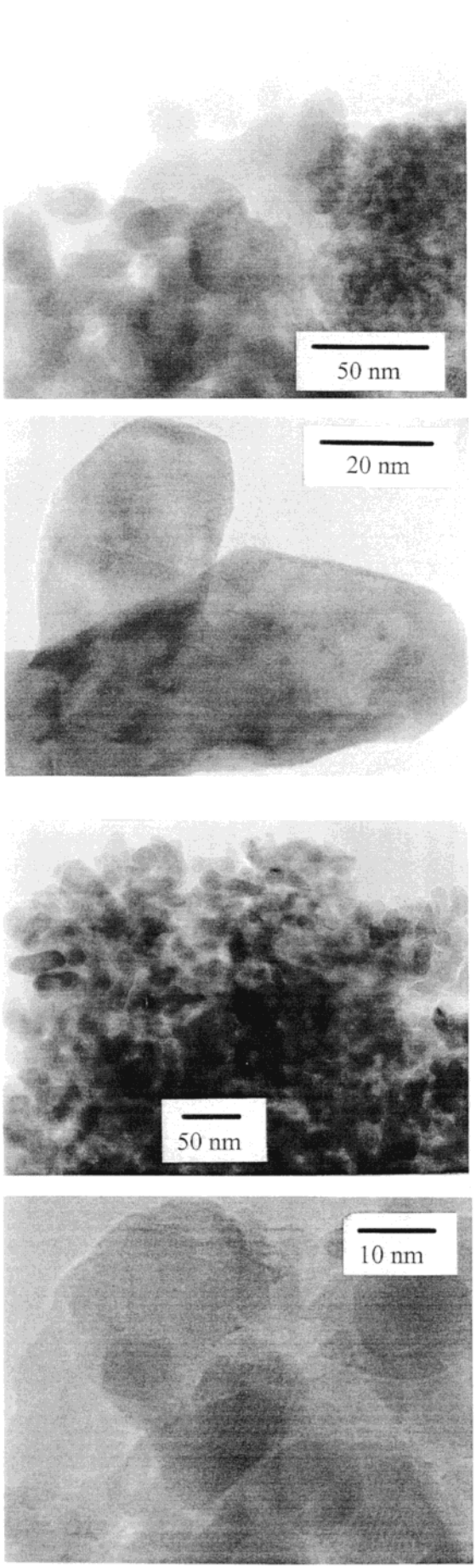

Figure 5. (HR)TEM images for pure (part A) and 8%-sulfated Fe_2O_3 (part B).

(15) Brunauer, S.; Hemmet, P. H.; Teller, E. *J. Am. Chem. Soc.* **1938**, *60*, 309.
(16) Barrett, E. P.; Joyner, L. S.; Halenda, P. P. *J. Am. Chem. Soc.* **1951**, *73*, 373.
(17) Farrow, R. L.; Nagelberg, A. S. *Appl. Phys. Lett.* **1980**, *36* (12), 945.
(18) Scheithauer, M.; Bosch, E.; Schubert, U. A.; Knözinger, H.; Cheung, T.-K.; Jentoft, F. C.; Gates, B. C.; Tesche, B. *J. Catal.* **1998**, *177*, 137.
(19) Yamamoto, T.; Tanaka, T.; Takenaka, S.; Yoshida, S.; Onari, T.; Takahashi, Y.; Kosaka, T.; Hasegawa, S.; Kudo, M. *J. Phys. Chem. B* **1999**, *103*, 2385.
(20) Morterra, C.; Cerrato, G.; Ardizzone, S.; Bianchi, C. L.; Signoretto, M.; Pinna, F. *Phys. Chem. Chem. Phys.* **2002**, *4*, 3136.
(21) JCPDS Table no. 6-0502.
(22) Unmuth, E. E.; Schwarth, L. H.; Butt, J. B. *J. Catal.* **1980**, *61*, 242.

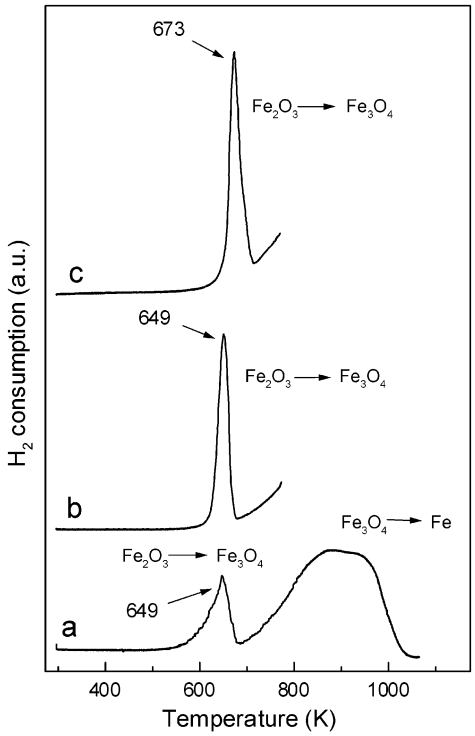

Figure 6. TPR profiles for Fe_2O_3 (curve a); Fe_2O_3 2% SO_4 (curve b); and Fe_2O_3 8% SO_4 (curve c).

of the overlapping decomposition/reduction of surface sulfates, and for this reason the curves relative to sulfated samples are limited to $T \approx 800$ K.

FTIR Characterization: Reducibility and Surface Functionalities. It is known that in situ FTIR spectroscopy can reveal the presence and features of surface functionalities and, in some cases, also the transformations occurring on the samples as a consequence of vacuum thermal activation treatments.

TPR analysis of Figure 6 indicated that, in the presence of hydrogen, pure Fe_2O_3 is reducible, in a two-stage process, first to Fe_3O_4 and eventually to Fe^0. It is also known that, on several oxidic systems, prolonged thermal treatments in vacuo can cause comparable reducing effects.

The IR spectra in Figure 7A, relative to the pure crystalline oxide activated in vacuo at RT, 473 K, and 573 K, show pronounced changes. The spectral features vary with continuity from those typical of a highly hydrated stoichiometric oxide (curve a) to those of a (semiconducting) reduced material (curve c), in which all vibrational structure is lost as a consequence of a total continuum absorption of the IR radiation, caused by electronic transitions. After thermal treatment at 473 K (curve b), abundant hydrocarbonaceous residues become evident in the spectrum. This phenomenon is often observed in the IR spectra of oxidic materials that were exposed to the atmosphere after a preparative step carried out at high temperatures, as the "activated" materials tend to adsorb from the atmosphere species that can be then transformed into carbonaceous residues and/or adsorbed CH_n groups. The latter can undergo a vacuum pyrolysis process and be, at least in part, responsible for a self-reductive process, as observed in some cases (e.g., see ref. 23). And, in fact, curve d of Figure 7A shows that the elimination of the surface CH_n residues, carried out with a preliminary burnoff in oxygen at 673 K, prevents the drastic reduction of Fe_2O_3 which, after vacuum treatment at 573 K, still exhibits the typical spectral features of a (quasi)-stoichiometric oxide. (Note that the weak evidence for CH_n species still present in spectrum d of Figure 7A, and in other spectra run after a burnoff treatment (e.g., see Figure 7B), is

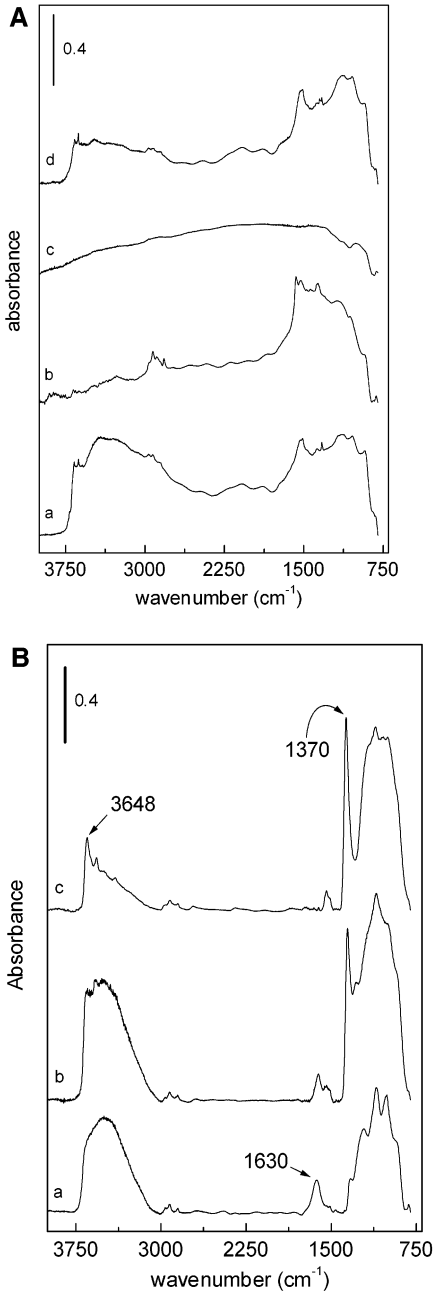

Figure 7. Absorbance background IR spectra obtained with thin layer deposition samples of pure Fe_2O_3 (part A) and 8%-sulfated Fe_2O_3 (part B), vacuum activated for 1 h at RT (curves a), 473 K (curves b), and 573 K (curves c). The spectrum d in part A was obtained by activating at 573 K a plain Fe_2O_3 sample that underwent a preliminary in situ oxidative treatment (with pure O_2) at 673 K, and then a thorough in situ rehydration (with saturated water vapor) at ambient temperature.

(23) Morterra, C.; Giamello, E.; Cerrato, G.; Centi, G.; Perathoner, S. *J. Catal.* **1998**, *179*, 111.

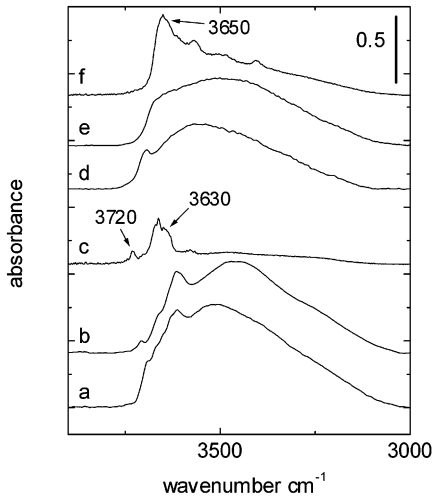

Figure 8. Absorbance background IR spectra in the ν_{OH} spectral region relative to: pure iron oxide in the presence of 1 Torr air (curve a), after evacuation at RT for 1 h (curve b), and after oxidative activation at 673 K (curve c); and 8%-sulfated iron oxide in the presence of 1 Torr air (curve d), after evacuation at RT for 1 h (curve e), and after oxidative activation at 673 K (curve f).

due to impurities always present on the IR windows, and easy to eliminate from the sample spectrum by subtraction of the empty-cell spectrum).

Figure 7B reports the background spectra relative to the iron oxide system with the highest sulfates loading. It can be seen that, on increasing the activation temperature, surface sulfates pass from a highly ionic form, characterized by an ill-resolved envelope of S−O bands located at $\bar{\nu} < 1350$ cm^{-1}, to a covalent form, characterized by a sharp band located at 1370−1380 cm^{-1} (the $\nu_{S=O}$ mode) and a complex envelope at $\bar{\nu} < 1250$ cm^{-1} (the ν_{S-O} modes). This spectral behavior with surface hydration is typical of surface sulfates on several ionic oxides (e.g., see ref. 24). More important, it is noted that in the presence of appreciable amounts of sulfates, the self-reductive process of iron oxide is inhibited. In fact, in every activation step carried out in vacuo, sulfated Fe_2O_3 shows the typical spectral features of a stoichiometric material, gradually brought from a state of high hydration (activation at RT, curve a; note the strong band at ∼1630 cm^{-1} due to the δ_{HOH} mode of coordinated water) to a medium-high dehydration stage (activation at 573 K, curve c). The explanation for this phenomenon can be as follows: thermally stable and highly acidic anionic species (sulfates, in this case), grafted to surface cationic centers, modify the reactivity of surface O^{2-} species, and doing so immobilize the surface species which could be lost by the starting Fe_2O_3 material in the self-reductive process brought about by vacuum treatments (and/or by the pyrolytic decomposition of hydrocarbonaceous residues, if still present).

The presence of sulfate groups modifies also the OH stretching profile of Fe_2O_3, as indicated by the comparison of the ν_{OH} spectral region of pure and highly sulfated systems reported in Figure 8. In the highly hydrated form, pure and sulfated samples exhibit almost the same spectroscopic behavior, and the spectrum of both systems is dominated by H-bonding interactions among OH-containing species. But many differences are observed after activating the samples at medium-high temperatures. In fact, the pure Fe_2O_3 sample dehydrated in oxidizing conditions at 673 K exhibits a typical spectrum, previously described by Rochester et al.[25] and by Busca et al.:[26] a weak signal at ∼3720 cm^{-1}, and a complex absorption at ∼3630 cm^{-1}, ascribable to terminal and bridged OH groups, respectively. A broad absorption observed by Busca et al. at ∼3460 cm^{-1},[26] and assigned to H-bonded OH groups present in micropores deriving from the precursor goethite, is not visible in the present case (curve c), in which no evidence for a microporosity was ever revealed by the *t*-plot method.[27]

After activation at 673 K, the sulfated system (curve f) shows a strong and complex absorption centered at $\bar{\nu} < 3700$ cm^{-1} (apparent maximum at ∼3650 cm^{-1}), tailed to the low-frequency side. This indicates the following: (i) the absence of terminal OH groups, usually absorbing at $\bar{\nu} > 3700$ cm^{-1}.[28] This is probably caused by a selective reaction of terminal OH species (more basic in nature) with the sulfating agent, to yield surface-grafted sulfate groups; (ii) a more hydrophilic nature for the sulfated material. In fact, in the presence of sulfates, a larger amount of surface hydroxyls remain, and some of the surface OH groups are still involved in H-bonding. The presence of (hydrophilic) surface sulfate groups was observed to induce similar effects also in other ionic oxidic systems.[29]

FTIR Spectroscopy: Surface Basicity. RT adsorption of CO_2 has been used to test the surface basicity of Fe-based systems activated in vacuo at 673 K.

It is known[30] that CO_2 can be adsorbed at the surface of oxidic materials in two ways: (i) linearly, when acting as a Lewis base. The interaction occurs through one of the oxygen atoms, with coordinatively unsaturated (cus) Lewis acid sites; and (ii) in a bent form, when acting as a weak acid. The interaction occurs by accepting electronic charge on the carbon atom from Lewis basic sites, such as surface O^{2-} ions, and giving rise to surface carbonate-like species. When CO_2 adsorption in a bent form involves surface OH^- groups, the resulting surface groups are the so-called bicarbonate-like species. Carbonate and bicarbonate species are characterized by a well-determined stretching frequency range for the symmetric and antisymmetric modes of the O−C−O group. In addition, bicarbonate species are often identified by the presence of the δ_{OH} mode at ∼1230 cm^{-1}, and of the corresponding ν_{OH} mode at ∼3610 cm^{-1}.[31]

(24) (a) Nakamoto, K. *Infrared and Raman Spectra of Inorganic and Coordination Compounds*, 2nd ed.; Wiley-Interscience: New York, 1970. (b) Bensitel, M.; Saur, O.; Lavalley, J.-C.; Mabilon, G. *Mater. Chem. Phys.* **1987**, *17*, 249. (c) Waquif, M.; Bachelier, J.; Saur, O.; Lavalley, J.-C. *J. Mol. Catal.* **1992**, *72*, 127.

(25) Rochester, C. H.; Tophan, S. A. *J. Chem. Soc., Faraday Trans. I* **1979**, 1073.

(26) Busca, G.; Lorenzelli, V. *React. Kinet. Catal. Lett.* **1980**, *15*, 273.

(27) (a) Lippens, B. C.; de Boer, J. H. *J. Catal.* **1965**, *4*, 319. (b) de Boer, J. H.; Linsen, B. G.; Osinga, Th. J. *J. Catal.* **1965**, *4*, 643. (c) Gregg, S. J.; Sing, K. S. W. *Adsorption, Surface Area and Porosity*; Academic Press: London, 1982.

(28) Tsyganenko, A. A.; Filimonov, V. N. *J. Mol. Struct.* **1973**, *19*, 579.

(29) Morterra, C.; Cerrato, G.; Pinna, F.; Signoretto, M.; Strukul, G. *J. Catal.* **1994**, *149*, 181.

(30) Little L. H. *Infrared Spectra of Adsorbed Species;* Academic Press: London, 1966.

(31) Busca, G.; Lorenzelli, V. *Mater. Chem.* **1982**, *7*, 89.

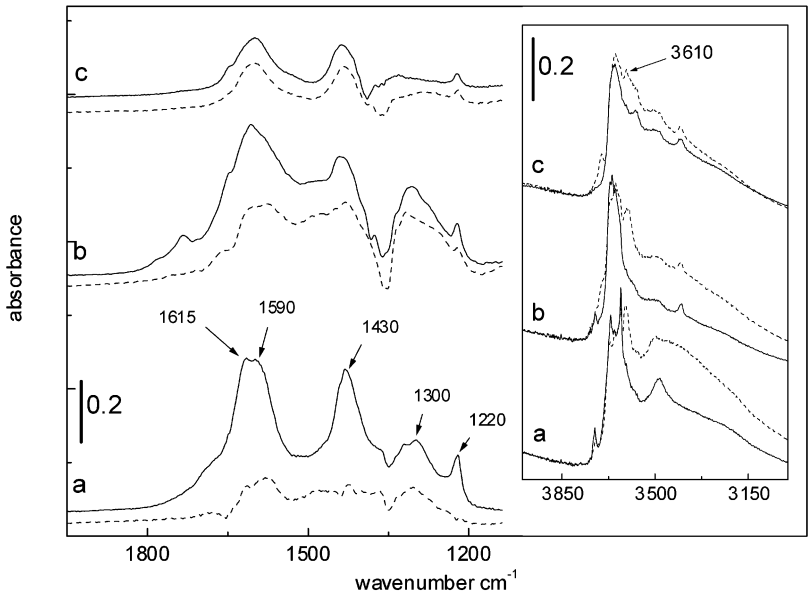

Figure 9. Differential absorbance IR spectra in the ν_{OCO} spectral region, relative to the adsorption of CO_2 on pure Fe_2O_3 (curves a), Fe_2O_3 2% SO_4 (curves b), and Fe_2O_3 8% SO_4 (curves c), activated in oxidizing conditions at 673 K. Solid-line curves: contact with 20 Torr CO_2; broken-line curves: after a 10 min evacuation at RT. Inset: the ν_{OH} spectral profile of the three samples, before (solid-line curves) and after (broken-line curves) CO_2 contact.

Figure 9 reports the differential spectra (i.e., after subtraction of the background spectrum of the bare solid) in the 2000−1000 cm^{-1} range obtained for the three materials under study after the contact with carbon dioxide and after CO_2 evacuation at RT. The use of differential spectra was necessary because the sample background spectra contained strong surface and bulk absorptions, deriving from the preparative process and clearly observable in Figure 7, that would interfere with the interpretation of the surface carbonate-like species formed upon CO_2 uptake.

Upon CO_2 uptake, several bands form that turn out to be largely reversible upon evacuation at RT (especially in the pure α-Fe_2O_3 sample of Figure 9a). The bands are ascribable to the following species:[31] (i) 1615 and 1430 cm^{-1} to the antisymmetric and symmetric ν_{OCO} modes of bicarbonates, together with the sharp band at 1220 cm^{-1}, due to the δ_{OH} mode (the high-frequency partner of this absorption is visible at ∼3600−3610 cm^{-1} in the inset); (ii) 1590 and 1300 cm^{-1} to the antisymmetric and symmetric ν_{OCO} modes of carbonates of the bidentate type. The assignment is based on the spectral separation between the two fundamental vibrations.[31]

The spectra of Figure 9 show that the formation of few bidentate carbonates and, far more abuntantly, of bicarbonate-like species is gradually decreased by the presence of surface sulfates, but not completely suppressed. This behavior is somewhat surprising, but not totally unexpected. In fact, the comparison between CO_2 adsorption on pure and sulfated zirconia[32] leads to the same conclusion: sulfate groups tend to graft on the oxide surface either through existing basic OH sites, or by converting the most basic oxygen atoms in a couple of OH groups. A reaction of condensation can then occur between the newly formed OH termination of the oxide and the sulfating agent. But even if sulfates do not cover the whole surface, so that surface oxygen sites still remain, the basicity of these sites is surely modified by the presence of nearby acidic surface sulfates, so that CO_2 cannot react to form carbonates and bicarbonates. Still, a very large amount of sulfates turns out to be needed to suppress (if at all) the activity toward CO_2. In this respect, it is recalled that the sulfates loading of the Fe_2O_3 8% SO_4 system (∼4.6 groups per nm^2, as reported in Table 1) is higher than that corresponding to a statistical sulfates monolayer (∼4 groups per nm^2 [33]). This datum, together with the still abundant presence of surface OH species (inset to Figure 9) indicates that the surface of iron oxide is virtually impossible to cover entirely with sulfate species and that, from a certain loading on, sulfates tend to assume a complex structure (polysulfates) rather than spreading on the whole surface.

FTIR Spectroscopy: Lewis and Brønsted Acidity. The adsorption of CO (both at RT and 77 K) and 2,6-dimethylpyridine has been used to test the surface acidity of our Fe_2O_3-based systems. All samples were vacuum activated in oxidizing conditions at 573 K (a medium-high activation temperature), to form a reasonable surface concentration of cus cationic sites (Lewis acid centers) and to leave, at the same time, a sufficient amount of residual OH functionalities (potential Brønsted acid centers).

CO Adsorption at RT. It is known that, in these experimental conditions and in the absence of processes other than a plain surface coordination, carbon monoxide acts as a weak Lewis base and can reveal the strongest fraction of surface Lewis acid sites. In fact, the lone pair in the weakly antibonding 5σ molecular orbital can be partly shared with a cus surface cationic site (through a partial σ-donation), yielding a slightly stronger C−O bond (i.e., an increase of the force

(32) Bolis, V.; Magnacca, G.; Cerrato, G.; Morterra, C. *Thermochim. Acta* **2001**, *379*, 147.

(33) Nascimento, P.; Akratopoulon, C.; Oszagyan, M.; Coudurier, G.; Travers, C.; Joly, J. F.; Vedrine, J. C. In *New Frontiers in Catalysis*; Guczi, L., Solymosi, F.,; Tétényi, P., Eds; Elsevier: Amsterdam, 1993; p 1185.

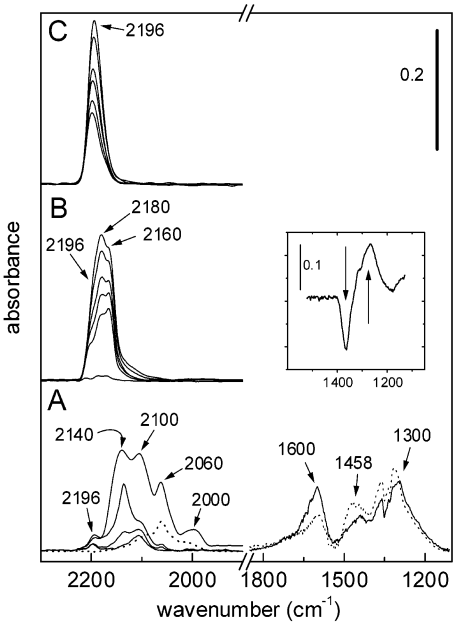

Figure 10. Absorbance IR spectra obtained in the 2300−1900 cm^{-1} range on increasing CO pressure (from 1 to ∼100 Torr) onto pure (part A), 2%-SO_4 (part B), and 8%-SO_4 (part C) iron oxide. The samples were activated/oxidized in situ at 573 K. The dotted-line trace in part A was obtained after CO evacuation at RT for 20 min. The low-ν subpart A (range: 1800−1150 cm^{-1}) reports the spectra obtained after 100 Torr CO contact (solid-line trace) and after 20 min evacuation at RT (dotted-line trace). The inset in part B shows the differential spectrum obtained in the $\nu_{S=O}$ spectral region after the admission of 100 Torr CO on the Fe_2O_3 2% SO_4 sample (activated/oxidized at 573 K): the negative peak (in respect of the zero-baseline) is relative to a signal disappearing upon CO uptake, and the positive peak is relative to a signal that increases upon CO uptake.

constant of the C−O oscillator). The response in the IR spectrum is an upward shift of the ν_{CO} mode with respect to the free gaseous molecule (2143 cm^{-1}), and the extent of the upward shift depends on the Lewis acidity of the adsorbing cationic sites. When the adsorbing cationic site has electrons in d atomic orbitals with appropriate symmetry, an additional π back-donation can occur, with an overall weakening of the C−O bond and consequent lowering of the ν_{CO} stretching frequency. In this case, the CO stretching frequency is no longer correlated with the Lewis acidity of the adsorbent, but can yield information on the oxidation state of the adsorbing sites.

Figure 10 compares the behavior of pure and sulfated Fe_2O_3 (activated/oxidized at 573 K) under the effect of increasing amounts of CO adsorbed at RT. In the high-ν part of section A, it can be observed that, on pure iron oxide, many bands form in a wide spectral range (2210−1960 cm^{-1}), and that their relative intensity depends on the coverage reached. In particular, is noted the presence of only a tiny component at frequencies higher than that of CO gas (∼2196 cm^{-1}), and visible in the spectrum only at relatively high coverages. The low-ν part of Figure 10A shows that, during CO uptake on pure α-Fe_2O_3, other bands form in the spectral range 1800−1200 cm^{-1}. The bands are due to surface carbonate-like species (mainly bidentates and monodentates[31]) and indicate that, on pure Fe_2O_3, the RT contact with CO brings about also a redox process that modifies the surface situation produced during the first activation/oxidation step. After an outgassing at RT (see the broken-line curves in Figure 10A), the only component left in the high-ν range absorbs weakly at ∼2060 cm^{-1}, indicating the presence of a strong π back-donation from the adsorbing metal ions to CO (reduced Fe), whereas in the low-ν range most carbonate-like species turn out to be irreversible to RT evacuation. After evacuation at RT, re-allowance of the maximum CO dose leads, in the high-ν range, to a complex spectrum that is virtually indistinguishable from that obtained in the first adsorption run under the same CO pressure. This indicates that both CO removal and second CO adsorption do not further modify the surface of the Fe_2O_3 specimen. The assignment of the carbonyl-like bands at $\bar{\nu}$ > 1900 cm^{-1} becomes somewhat easier considering the spectra obtained with the other samples. In the case of the 2% sulfate-promoted Fe_2O_3 specimen (section B), only few components are present at low wavenumbers (and none at $\bar{\nu}$ < 2143 cm^{-1}), whereas there are no bands at $\bar{\nu}$ < 2196 cm^{-1} in the case of the 8% sulfate-promoted sample (section C). It was shown above that the presence of sulfates inhibits the reducibility of iron oxide. Therefore the carbonyl component at 2196 cm^{-1}, whose relative intensity is strongly dependent on sulfates coverage, and is the only adspecies present on the high-loading material, should be assigned to CO adsorbed onto cus Fe^{3+} sites. In the case of pure iron oxide, the bands present at low wavenumbers should be ascribed to carbonyl-like species formed onto cus Fe^{n+} sites, where $0 \le n < 3$. Experiments carried out on systems containing supported iron (e.g., see refs. 34 and 35) allowed assignment of a component at ∼2100 cm^{-1} to CO−Fe^{2+} complexes, and assignment of a band at ∼1980 cm^{-1} to CO−Fe^0 species. It is also probable that bands at $\bar{\nu}$ < 2100 cm^{-1} may contain components ascribable to bridged CO adspecies.[30]

The picture deriving from CO uptake at RT thus indicates the following: (i) in the presence of appreciable amounts of surface sulfates, no reduced Fe centers are present after activation nor form upon CO contact, whereas a plain σ-donation to Fe^{3+} sites dominates; and (ii) in the absence of sulfates, large amounts of reduced Fe centers (down to Fe^0) are present and/or form, so that CO adsorption implies an appreciable and variable contribution of π-back-donation.

CO uptake at ambient temperature does not indicate whether reduced Fe sites are present at the surface of the iron oxide adsorbent before adsorption, or are produced during the adsorption process as a consequence of the reducing character of CO. Because the activation treatment at 573 K was carried out in oxidizing conditions, on the basis of what is reported in Figure 7 (and relevant discussion), we favor the second hypothesis. To make this point clear, the adsorption of CO at low temperatures has been resorted to, and is reported below.

A differential spectral segment, showing the modification occurring to the $\nu_{S=O}$ signal in the presence of adsorbed CO, has been inserted in Figure 10B. CO molecules are not thought to interact directly with sulfuryl groups, but (charge-release) electronic effects

(34) Schreiber, K. C. *Anal. Chem.* **1949**, *21*, 1168.
(35) Colthup, N. B. *J. Opt. Soc. Am.* **1983**, *40*, 307.

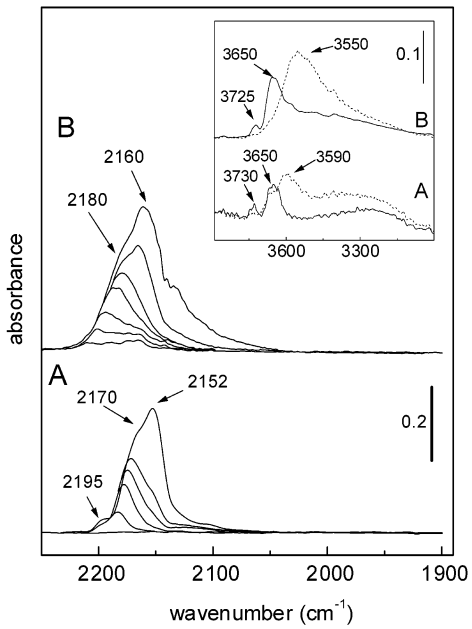

Figure 11. Absorbance IR spectra obtained at ~77 K upon adsorption of 20 Torr CO onto pure Fe_2O_3 (part A), and 8%-SO_4 Fe_2O_3 (part B), followed by a stepwise desorption to 1×10^{-3} Torr at the same temperature. The samples were activated at 573 K in oxidizing conditions. Inset: ν_{OH} spectral profile relative to the two samples before (solid-line curves) and after (broken-line curves) 20 Torr CO adsorption at 77 K.

cause a partial rearrangment of sulfate groups and, consequently, the $\nu_{S=O}$ band shifts. This spectroscopic effect will turn out to be important in the comprehension of some microcalorimetric results (see below), in which unexpectedly low adsorption heat values are obtained upon CO uptake.

CO Adsorption at 77 K. In these experimental conditions, high CO coverages (virtually up to $\theta \approx 1$) are reached, and all types of interaction between CO and surface sites can be evidenced. Moreover, the reducing activity of CO toward reducible surface species should be largely suppressed by the low temperature. Figure 11 is relative to CO adsorption at 77 K on the systems Fe_2O_3 (section A) and Fe_2O_3 8% SO_4 (section B). In both cases, only two main absorptions at $\bar{\nu} > 2143$ cm^{-1} are observed. For unpromoted Fe_2O_3, the main spectral feature is a strong band at ~2170 cm^{-1} with a high-wavenumber (satellite) minor component at ~2195 cm^{-1}. In view of the high-ν spectral position, both bands are ascribed to CO molecules interacting with (two families of) cus Fe^{3+} cations. It is recalled that only the high-ν component (~2195 cm^{-1}) was (partially) visible upon CO adsorption at RT in Figure 10A. Moreover, there is a low-wavenumber band (~2150 cm^{-1}), strongly dependent on CO pressure, that is ascribed to the H-bonding interaction of CO with surface OH groups. The assignment is confirmed by the two curves in the inset (section A), where in the ν_{OH} region is clearly visible a weak OH perturbation, brought about by CO uptake ($-\Delta\bar{\nu}_{OH} \approx 70-140$ cm^{-1}).

In the case of sulfated iron oxide (section B of Figure 11), both CO bands (i.e., coordinated and H-bonded CO) show an upward-shift of ~10 cm^{-1}, which can be ascribed, for the high-wavenumber band, to an enhanced electron-withdrawing power of Lewis acid sites produced by surface sulfate groups and, for the low-wavenumber band, to the probable presence of a protonic (Brønsted) acidity, yielding stronger H-bonding interactions with CO. The stronger H-bonding system is confirmed by the larger half-bandwidth and downward shift of the OH band in section B of the inset to Figure 11 ($-\Delta\bar{\nu}_{OH} \approx 100-175$ cm^{-1}).

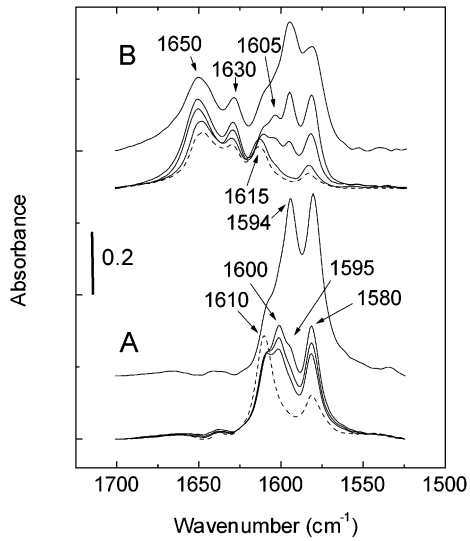

Figure 12. IR spectra obtained upon 2,6-dimethylpyridine adsorption (top spectra), and subsequent evacuation for 1 min, 5 min, and 15 min at beam-temperature (BT), and 15 min at 423 K (broken-line curves) on pure Fe_2O_3 (part A) and on 8% SO_4 Fe_2O_3 (part B). Both samples were activated in oxidizing conditions at 673 K.

The assignment involving the presence of Brønsted acid sites must be confirmed, and to this goal Brønsted acidity has been checked by the adsorption of 2,6-dimethylpyridine, reported in the next section.

2,6-Dimethylpyridine (DMP) Adsorption at RT. Figure 12 reports the spectra obtained after adsorption/evacuation of 2,6-DMP on pure and highly sulfated iron oxide activated/oxidized at 673 K. The experiment was mainly carried out to determine whether sulfate groups can develop Brønsted acidity at the surface of iron oxide, as they do at the surface of other oxidic systems.[36] The activated samples were contacted with 2,6-DMP (saturated vapor pressure), and then the coverage of the adsorbed phase was decreased by pumping off for increasing times at the temperature of the IR beam (BT), and eventually by heating the samples in vacuo at 423 K (15 min).

As discussed elsewhere,[37] with 2,6-DMP adsorption the most useful analytical spectral range in the mid-IR region (1700−1500 cm^{-1}) comprehends the bands due to the 8a−8b modes of the adsorbate. Spectral position and lability of the bands assist in the assignment of the various components. The spectral region of interest can be divided into two parts: at $\bar{\nu} < 1625$ cm^{-1} fall the 8a−8b components due to molecular 2,6-DMP, whereas at $\bar{\nu} > 1625$ cm^{-1} fall the 8a−8b components due to lutidinium ions (and thus related to the presence of Brønsted acidity). In particular: (i) a band at ~1580 cm^{-1} is assigned to the 8b mode of both chemisorbed and liquidlike (physisorbed) 2,6-DMP, and corresponds

(36) Arata, K.; Hino, M. *Appl. Catal.* **1990**, *59*, 197.
(37) Morterra, C.; Cerrato, G.; Meligrana, G. *Langmuir* **2001**, *17*, 7053.

to the total amount of molecular 2,6-DMP at the oxide surface; and (ii) the bands between 1590 and 1620 cm^{-1} are due to the 8a mode of adsorbed 2,6-DMP species, and, superimposed on them, a strongly pressure-dependent component at ∼1595 cm^{-1} is the 8a mode relative to the liquidlike (physisorbed) 2,6-DMP phase. As for specifically adsorbed 2,6-DMP species (8a mode in the 1590−1620 cm^{-1} range), increasing adsorption strength increases the frequency of the 8a vibrational mode. The weakest specific interaction expected is of the H-bonding type (interaction between 2,6-DMP and some surface OH groups), and the relevant 8a absorption is observed in Figure 12 at ∼1595 cm^{-1} (i.e., distinguishable from physisorbed 2,6-DMP only for a higher resistance to evacuation). Stronger interactions are due to 2,6-DMP adsorbed on two families of Lewis acidic sites: the relevant 8a absorptions are observed in Figure 12 at ∼1600 and ∼1610 cm^{-1} (part A), or ∼1605 and ∼1615 cm^{-1} for sulfated Fe_2O_3 (part B), respectively. In particular, the decreasing coverage caused by outgassing at BT and 423 K, respectively, leaves on both specimens only the 8a component at 1610−1615 cm^{-1}, which corresponds to the adsorption on the strongest fraction of Lewis acid sites present at the surface of the oxide.

The sulfated sample of Figure 12B shows other two components at $\bar{\nu} > 1625$ cm^{-1}, which are relative to the 8a−8b vibrational modes of lutidinium adspecies (∼1630 and ∼1650 cm^{-1}, respectively), indicating that (i) also on iron oxide the presence of sulfate groups is active in developing a protonic Brønsted acidity, and that (ii) also after activation at 673 K (medium-high dehydration degree) an appreciable amount of surface OH species still possess a Brønsted acidic character.

The comparison of the spectra relative to 1-min evacuation at BT of 2,6-DMP from the two samples allows evaluation of the different amount of strong Lewis acid sites. In fact, comparing the two spectra obtained under similar 2,6-DMP residual pressure (note the similar intensity of the 8b component at 1580 cm^{-1}), it appears quite clearly that the uptake onto Lewis acid sites (1605−1615 cm^{-1}) is definitely lower on the sulfated system than on the unsulfated one (1600−1610 cm^{-1}). At the same time, the higher spectral position of the 8a mode indicates that (the residual) Lewis acid sites at the surface of sulfated iron oxide are stronger than those on the pure oxide. The results are not surprising, as it has been already observed on other sulfated systems (e.g., see ref 38) that the presence of sulfate groups reduces the amount of Lewis acidity (as sulfates are thermally stable at the activation temperatures adopted, and thus fewer cus cationic sites are created upon dehydration), but the residual Lewis acidity is stronger, due to inductive effects from the charge-withdrawing surface sulfates.

Adsorption Microcalorimetry: Quantitative and Energetic Features of CO Adsorption at 303 K. The combined use of adsorption microcalorimetry and FTIR spectroscopy applied to the study of probe molecules adsorption is quite useful in determining the surface behavior of adsorbents. In fact, FTIR spectroscopy yields qualitative information on the nature of adsorbed species, whereas adsorption microcalorimetry follows the adsorption process in quantitative and energetic terms.

Here, we studied the adsorption of CO at ambient temperature (303 K) to analyze in quantitative terms both the strong Lewis acidity of pure and sulfate-doped α-Fe_2O_3, previously studied by IR spectroscopy (see Figure 10), and some aspects of the surface reducibility of the materials.

The quantitative approach is usually based on simultaneously obtaining volumetric adsorption isotherms (yielding adsorbed/consumed amounts of the adsorptive) and calorimetric isotherms (yielding evolved heats). Both types of isotherms are usually obtained in two (or more) consecutive runs, separated by a thorough evacuation at the adsorption temperature. The difference between the first run (primary isotherms) and the second run (secondary isotherms) represents, both in terms of adsorbed/consumed amounts and of released heats, the irreversible component of the first contact process. Needless to say, if differences are still observed (or not observed) between secondary isotherms and the isotherms of further runs, quantitative information is gained on the persistence (or nonpersistence) of irreversible surface processes. As for the energetic aspects of the adsorption phenomena, useful energetic details are usually obtained by combining volumetric and calorimetric isotherms, so that plots of (differential) molar adsorption heats can be constructed as a function of increasing surface coverage.

Some of the quantitative and energetic results relative to CO uptake on pure and sulfate-promoted Fe_2O_3 systems are reported in Figure 13.

Volumetric isotherms (part A) indicate the following. (i) As expected, CO uptake decreases fast with increasing sulfates loading, meaning that as increasing fractions of the surface become occupied by stable anionic species,[9] less and less cus surface active sites can be produced upon thermal activation. Still, the secondary adsorption isotherm of pure Fe_2O_3 (corresponding, as reported below, to plain and reversible CO uptake on cus surface centers) lies lower than the adsorption isotherms on the low-loading 2%-SO_4 sample. This apparent contradiction is a first indication that, in the first adsorption run on pure Fe_2O_3, other processes occur (such as, for instance, surface reduction by CO), leading to the formation of irreversible surface species that, in the secondary adsorption run, will compete with the plain CO coordination process. And, in fact, the inset to Figure 10A showed that the first contact with CO produces appreciable amounts of surface bidentate carbonate-like species that adsorb irreversibly at surface cus cation−anion couples. (ii) CO adsorption turns out to be completely reversible for the two sulfated Fe_2O_3 systems, in agreement with IR data of Figure 10, indicating that CO is adsorbed with formation of a purely σ-dative bond. Unlike that, in the primary adsorption run on pure iron oxide, more than 50% of CO molecules are irreversibly consumed. This is the consequence of the occurrence of two processes, as already mentioned above: the reduction of reducible surface sites (which consumes CO molecules and yields surface carbonates), and a strong adsorption via both σ-donation and π-back-donation onto Fe^{n+} sites (with $n < 3$). The oxidative irreversible consumption of CO on

(38) Morterra, C.; Cerrato, G.; Emanuel, C.; Bolis, V. *J. Catal.* **1993**, *142*, 349.

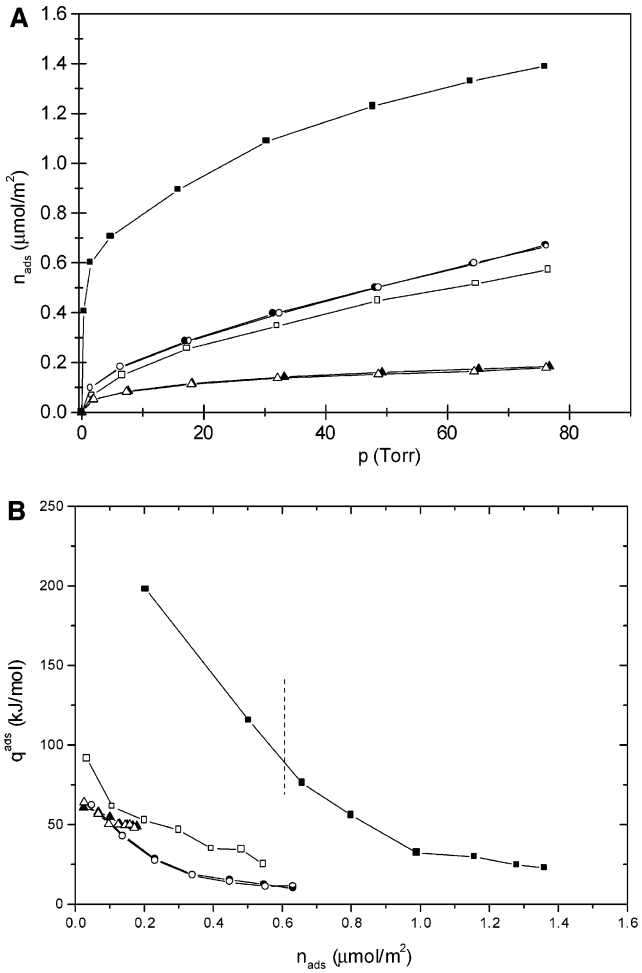

Figure 13. Plots of primary (solid symbols) and secondary (open symbols) volumetric isotherms (part A), and (differential) molar adsorption heats vs coverage (part B), obtained for CO adsorption at 303 K. Squares, adsorption onto Fe_2O_3; circles, adsorption onto Fe_2O_3 2% SO_4; triangles, adsorption onto Fe_2O_3 8% SO_4. All samples were activated in oxidizing condition at 573 K, to compare these data with the IR data of Figure 10.

pure Fe_2O_3 seems to occur in the very first fraction of the adsorption process. In fact, the primary (pseudo-) adsorption isotherm exhibits a very steep initial part (leading to the consumption of ~0.6 μmol CO per nm^2 at $p_{CO} \approx 0$), followed by a second Langmuir-like part. The latter runs quite parallel to the corresponding secondary (real-) adsorption isotherm, and both are due to the small fraction of sites available for a plain reversible CO coordination. It is important to note that this sites fraction, responsible for the secondary isotherm, is "stable", as a third adsorption run (not shown) reproduces the secondary isotherm, confirming the reproducibility of the secondary adsorption process already evidenced by IR spectra. (iii) Only for the sample doped with the highest sulfates loading, the Langmuir-like CO uptake reaches a plateau within $p_{CO} \approx 60$ Torr, indicating that complete coverage of the available surface sites is reached fast, whereas for both low SO_4^{2-} loading and unpromoted Fe_2O_3 (secondary isotherm) part of the surface sites are still accessible to CO adsorption at the highest CO pressure explored ($p_{CO} \approx 80$ Torr).

Heat of adsorption plots, reported in Figure 13B in the form of differential molar heats vs surface uptake, indicate the following. (i) The (reversible) secondary adsorption run on nonsulfated Fe_2O_3 and both adsorption runs on the low-loading sulfated material present an appreciable decrease of q^{ads} with surface coverage, corresponding to a vast sites heterogeneity. This situation is well reflected by the IR spectra of Figure 10A and B, where the presence of many CO components is clearly visible. The q^{ads} curves are completely different for the high-loading Fe_2O_3 8% SO_4 sample: all experimental points fall in a narrow heat range (50−70 kJ/mol) and, consistently, the IR spectra of Figure 10C indicate the presence of only one family of CO-adsorbing sites, absorbing at ~2196 cm^{-1}. Moreover, the minimal coverage extension of the q^{ads} curves confirms that, in the presence of the highest sulfates loading, only a few adsorbing sites are available for CO uptake at ~300 K. (ii) Values of q^{ads} are dramatically higher for the primary adsorption run on pure Fe_2O_3 than for the corresponding secondary run and for all sulfated systems, confirming that the primary CO contact with pure iron oxide does not yield a simple adsorption process, but involves a surface reduction reaction. In Figure 13A it was shown that, in the primary adsorption run, some 0.6 μmol CO is consumed at $p_{CO} \approx 0$, and most likely correspond to the Fe_2O_3 surface reduction step. The heat curve of Figure 13B confirms that, after 0.6 μmol CO is consumed in the primary adsorption run, q^{ads} figures fall below ~100 kJ mol^{-1} and, after that, the heat curve keeps declining quite parallel to the curve of the plain surface coordination in the secondary run. In fact, when reducible sites are reduced by the first CO molecules, the "stable" secondary adsorption run occurs releasing adsorption heats of the right order of magnitude for CO adsorbed on most oxidic systems (e.g., see ref. 39).(iii) The heats of adsorption on sulfated systems present peculiar aspects that deserve some comments. The q^{ads} curves of both sulfated systems start at heat values (q^0) definitely lower than that of the secondary run on plain Fe_2O_3, and at high CO coverage the q^{ads} curves of the low-loading Fe_2O_3 2% SO_4 system reach extremely low values (~10 kJ mol^{-1}), still definitely lower than those of the secondary run on plain Fe_2O_3. The first aspect could be consistent with the virtual absence or scarce presence, in the presence of sulfates, of π back-donation contribution in CO uptake, but is certainly not consistent with the presence of surface sulfates that are known to induce, by inductive effects, an increase of the Lewis acidity of surface cationic sites (e.g., see ref. 37). As for the second aspect, at 303 K heat values as low as ~10 kJ mol^{-1} are not easily explainable in terms of a σ-donation from CO to cus cationic sites (as charge-withdrawing sites of low-energy should not be able to adsorb CO at 303 K). It is possible that the q^{ads} curves that correspond to the always exothermic adsorption process are kept so low by the co-presence of an endothermic surface process. In other cases, such as, for instance, the adsorption of CO onto γ- and δ,θ-Al_2O_3[40] the observation of low adsorption enthalpies at high coverage was suggested to be caused by the co-presence of an endothermic "reconstruction" effect produced by CO on the surface of the material, and the

(39) Bolis, V.; Magnacca, G.; Morterra, C. *Res. Chem. Intermed.* **1999**, *25* (1), 25.
(40) Morterra, C.; Bolis, V.; Magnacca, G. *Langmuir* **1994**, *10*, 1812.

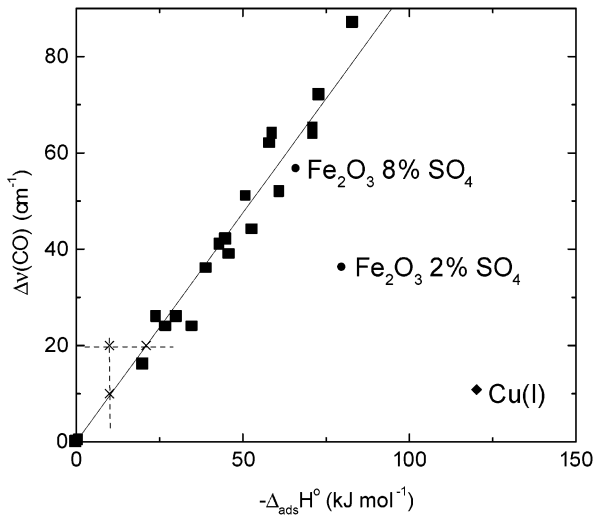

Figure 14. Correlation diagram (as reported in ref. 39) showing, for adsorbed CO, the upward frequency shift with respect to free CO gas (2143 cm^{-1}) as a function of the corresponding heats of adsorption, both extrapolated to zero-coverage. Data refer to the adsorption at 303 K of CO on various d^0 oxidic adsorbents (squared symbols), on a non-d^0 oxidic system (Cu_2O;[41] diamond symbol), and to some of the present Fe_2O_3-based systems (round symbols). The broken-line traces and the cross symbols in the lower part of the plot concern the high-coverage behavior of the low-loading Fe_2O_3 2% SO_4 system (see text).

occurrence of that reversible process could be demonstrated spectroscopically. In the present case, no spectral changes are observed in the surface component(s) of bulk vibrational modes. Moreover, the heat-lowering effect is much smaller than in the case of aluminas and concerns only the sulfate-doped Fe_2O_3 systems. It is therefore believed that here the heat-lowering effect is caused by the occurrence of a reversible change of coordination of surface sulfates, induced by the charge-releasing CO uptake. This is indeed demonstrated by the downward shift of the high-frequency $\nu_{S=O}$ mode, shown in the inset to Figure 10B.

In this respect, it may be useful to compare spectroscopic and energetic data of CO uptake on Fe_2O_3 systems, using the correlation diagram shown in Figure 14, and reporting the spectroscopic shift observed for adsorbed CO (with respect to the gas molecule) versus the adsorption entalpy, both extrapolated to zero coverage. This diagram was obtained using data collected during the past few years for CO adsorbed on various oxidic adsorbents (see ref. 39). Note that the experimental points fit within a linear correlation whenever a pure σ-dative bond between CO and the adsorbing site is involved. (And, in fact, the point relative to the adsorption of CO onto Cu(I) oxide, reported for comparison, falls well off the linear correlation plot[41]).

The q^{ads} value observed at high CO coverage for the Fe_2O_3 2% SO_4 system and indicated in the figure by the cross symbol (~10 kJ mol^{-1}) would be well correlated with a $\Delta\bar{\nu}_{CO}$ shift of ~8 cm^{-1}, corresponding to an IR signal at ~2150 cm^{-1}, i.e., a frequency never observed for the RT σ-coordinative CO adsorption on oxides. The IR spectra of the present system indicate that the lowest-ν CO component, still forming at high coverages, absorbs at ~2160 cm^{-1} ($\Delta\bar{\nu}_{CO} \approx 17$ cm^{-1}), a shift value still reasonably correlated with the adsorption energy measured, but certainly much better correlated with the heat value ($q^{ads} \approx 20$ kJ mol^{-1}) observed for the asymptotic value of the secondary adsorption on pure Fe_2O_3, where no spectral perturbation on sulfates is present and where the last CO adspecies forming at high coverages do contain spectral components at ~2160 cm^{-1}.

Trying to correlate, on the basis of the correlation diagram of Figure 14, the $\Delta\bar{\nu}_{CO}$ and q^{ads} figures extrapolated to zero coverage for our iron-based materials, the points reported in the figure with round symbols are obtained. Only the result obtained for the system with the highest SO_4-loading is in good agreement with the correlation plot, confirming the virtual absence of reduction and/or π-back-donation already suggested by the spectral pattern of Figure 10C. Still, the real q^{ads} value should be somewhat higher (i.e., somewhat on the right of where the point is shown in the plot), because also at zero coverage the endothermic perturbation effect on surface sulfates is expected to be present. As for the point obtained for the low-loading Fe_2O_3 2% SO_4 system, it is not very far from the correlation line but certainly does not fit it, confirming the indication of the spectral pattern of Figure 10B, in which the presence of components ascribable to slightly reduced Fe species was suggested. Needless to say, the points obtained for both primary and secondary adsorption on the pure Fe_2O_3 system are completely out the considered range, as the zero-coverage phase of the primary uptake is dominated by the reduction process, and that of the secondary uptake is dominated by CO adsorption on reduced Fe^{n+} centers, i.e., by the presence of abundant π-back-donation.

Conclusions

As already discussed for other oxidic systems, it has been found that surface sulfation causes deep modifications in the behavior of iron oxide. The modifications do not involve the crystallographic structure of the oxide (that remains in the α-phase, both in the bulk and at the surface), but concern both morphological (physical) and chemical aspects. More in detail, physical changes derive from the fact that surface sulfation inhibits the growth of the particles and increases the total porosity decreasing the pore average size.

As for the chemical aspects, the changes are quite drastic, and involve several aspects of the reactivity of the oxide, namely the following: (1) surface basicity, as tested by CO_2 adsorption. Gradually, the introduction of sulfate groups tends to suppress the basic activity toward CO_2; (2) Brønsted acidity. When Fe_2O_3 is loaded (also partially) with sulfates, the system developes a protonic (Brønsted) activity that is never present in the pure oxide. (3) The most important change concerns the (surface) reducibility of the oxide. Surface sulfation immobilizes the most labile surface oxygen ions and hinders self-reductive processes. Reduction phenomena can be induced by mild reducing agents such as CO at RT, and the redox process is witnessed by the abundant formation of surface carbonate-like groups. But reduction can be caused also by simple activation in vacuo at

(41) Bolis, V.; Bordiga, S.; Graneris, V.; Lamberti, C.; Turnes Palomino, G.; Zecchina, A. *Stud. Surf. Sci. Catal.* **2000**, *130*, 326.

medium-high temperatures, especially when hydrocarbonaceous contaminants are present at the surface of the material.

When the material undergoes self-reduction effects, the nature of the Lewis acidic sites also changes dramatically: Fe^{3+}_{cus} sites are reduced to Fe^{n+}_{cus} (with $n < 3$), and reduced cationic sites can give π-back-donation with the probe CO molecules.

The combined use of in situ FTIR spectroscopy and adsorption microcalorimetry for CO adsorption on high-loading sulfated iron oxide (the Fe_2O_3 8% SO_4 system), where the system is rendered nonreducible and CO uptake yields a simple σ-coordination, allows addition of one more point in the correlation diagram $\bar{\nu}_{CO}$ vs heats of adsorption (at zero coverage) obtained in the last years for various oxidic adsorbents.

Acknowledgment. We thank Dr. A. Frache for registration of Raman spectra and Mr. S. Tripodi for carrying out most of the spectroscopic and microcalorimetric experiments. Some data from microcalorimetric experiments were discussed with Prof. V. Bolis and her contribution is gratefully acknowledged. This research was partly financed by the Italian Murst, project Cofin 2000, section 03.

CM021268N